



## Removal of $\text{Cu}^{2+}$ from aqueous solution by Chitosan/Rectorite nanocomposite microspheres

Tao Feng<sup>a,\*</sup>, Jie Wang<sup>a</sup>, Xiaowen Shi<sup>b</sup>

<sup>a</sup>College of Resources and Environmental Engineering, Wuhan University of Science and Technology, Wuhan 430081, China

Tel./Fax: +86 27 68862875; email: fengtaowhu@163.com

<sup>b</sup>Hubei Biomass-Resource Chemistry and Environmental Biotechnology Key Laboratory, Wuhan University, Wuhan 430079, China

Received 27 January 2013; Accepted 1 June 2013

### ABSTRACT

The novel chitosan/rectorite nanocomposite microspheres were prepared by controlling mass ratios of chitosan and rectorite at 6:1. The microspheres were characterized by Fourier transform infrared spectrophotometer, X-ray diffraction, and scanning electron microscope. The interlayer distance of rectorite was enlarged from 2.53 to 3.01 nm. Adsorption of  $\text{Cu}^{2+}$  from aqueous solution onto chitosan/rectorite nanocomposite microspheres was studied. The results showed that the  $\text{Cu}^{2+}$  adsorption process is dependent on pH, contact time, initial CR concentration, and temperature. The maximal  $\text{Cu}^{2+}$  uptake was  $190.2 \text{ mg g}^{-1}$  in the test. The adsorption kinetics, isotherms, and thermodynamics were also studied. The maximum sorption capacities calculated from the pseudo-second-order rate equation and Langmuir isotherm were 209.5 and  $201.6 \text{ mg g}^{-1}$ , respectively, which were close to the experimental values. Adsorption thermodynamics study indicated the spontaneous nature and endothermic of the adsorption process.

*Keywords:* Chitosan; Rectorite; Microspheres; Adsorption;  $\text{Cu}^{2+}$

### 1. Introduction

In recent years, the preparation of polymer/clay nanocomposites has attracted much attention because of their relative low production cost and obviously improved mechanical and materials properties. Due to polymer and clay combine the structure of physical and chemical properties of both organic and inorganic materials, polymer/clay nanocomposites exhibited excellent properties such as high storage modulus [1] and ionic conductivity [2]. Though polymer/clay nanocomposite has been widely studied, most reports concentrated on montmorillonite [3], seldom focus on rectorite (REC).

REC is a kind of layered silicate that the structure and characteristics are much similar to those of montmorillonite. It is referred as an interstratified clay mineral made of regular 1:1 stacking of dioctahedral mica-like layer (nonexpansible) and dioctahedral montmorillonite-like layer (expansible). The cations of  $\text{Na}^+$ ,  $\text{K}^+$ , and  $\text{Ca}^{2+}$  that lie in the interlayer region between 2:1 mica-like layers and 2:1 smectite-like layers can be exchanged easily by either organic or inorganic cations. Meanwhile, the separable layer thickness and layer aspect ratio (area-thickness) of REC are larger than those of regular montmorillonite [4]. These characteristics may be favorable for forming the intercalated or exfoliated composites and help to improve the efficiency of adsorption.

\*Corresponding author.

Chitosan is a high molecular weight polysaccharide composed of  $\beta$ -(1,4)-2-acetamido-2-deoxy-D-glucose and  $\beta$ -(1,4)-2-amino-2-deoxy-D-glucose units. It has many interesting characteristics such as hydrophilicity, biocompatibility, biodegradability, antibacterial properties, and flocculating regeneration ability. Also, the noxious heavy metal ions, such as Hg(II), Cu(II), Ni(II), and Cr(III), can be effectively removed through the  $-\text{NH}_2$  and  $-\text{OH}$  groups on the chitosan molecule. Due to these characteristics, chitosan has been widely used in many fields to remove dyes [5] and heavy metals [6,7] etc. To improve its adsorption ability, researchers introduced that the cationic biopolymer chitosan can be intercalated in rectorite through cationic exchange and hydrogen bonding processes. Monvisade and Siriphannon synthesized chitosan intercalated montmorillonite nanocomposite, which have been successfully used to remove cationic dyes [8]. Kittinaovarat et al. studied the adsorption activities of Reactive Red 120 onto chitosan/montmorillonite beads [9].

In the present work, chitosan/REC nanocomposite microspheres were prepared and characterized by X-ray diffraction (XRD), Fourier transform infrared spectrophotometer, and scanning electron microscope (SEM).  $\text{Cu}^{2+}$  was selected as a model metal ion to investigate the adsorption activity of heavy metal ions onto chitosan/REC nanocomposite microspheres. The effects of contact time, initial  $\text{Cu}^{2+}$  concentration, pH, and temperature on the adsorption were investigated in detail. The adsorption kinetics, isotherms, and thermodynamics were also studied.

## 2. Materials and methods

### 2.1. Materials

Chitosan was supplied by Zhejiang Ocean Biochemical Company. The degree of deacetylation as determined by potentiometric analysis was 90%, and the molecular weight calculated from GPC was  $2.3 \times 10^5$ . Calcium rectorite ( $\text{Ca}^{2+}$ -REC) refined from the clay minerals was provided by Hubei Mingliu Inc. Co. (Wuhan, China). Copper acetate, formaldehyde, epichlorohydrin, sodium hydroxide, glacial acetic acid, and other chemicals were of analytical grade. All solutions were prepared with distilled water.

### 2.2. Preparation of chitosan/REC nanocomposite microspheres

A 0.5 g REC was dipped in 10 mL distilled water and stirred for 6 h and then left standing for 24 h. Chitosan was dissolved in 1% (w/v) acetic acid to prepare the 0.5% (w/v) solution. The resulting solution

was added slowly into the pretreated REC suspensions under stirring at 60°C to obtain nanocomposite with initial chitosan/REC weight ratios of 6:1. The resulting mixture was precipitated with 10% (w/v) NaOH. The formed composites were filtered and washed with distilled water until the solution became neutral. Finally, the chitosan/REC nanocomposite microspheres were dried and ground to powder.

The nanocomposite was dissolved in 50 mL 2% (v/v) acetic acid and stirred for 4 h. It was then poured into the dispersion medium, which was composed of 50-mL liquid paraffin and an emulsifier (Span-80). The mixture was stirred for 30 min to form water in oil (w/o) dispersion and formaldehyde was added into the medium. After 2 h, the microspheres were collected and washed consecutively with ether, ethanol, and distilled water and then putted into an epichlorohydrin solution at 70°C for 3 h. Later, the microspheres were filtered and soaked overnight with 1% hydrochloric acid solution to remove formaldehyde. The microspheres were washed and then dried in an oven at 60°C for further analysis and use.

### 2.3. Characterization of chitosan/REC nanocomposite microspheres

The samples were grounded into powder for the preparation of KBr pellets. IR spectra of the powdered samples were recorded on Nicolet-360 FT-IR spectrometer with KBr pellet. The spectrum was corrected for the background noise.

The XRD experiment was performed using a diffractometer type D/max-rA (Tokyo, Japan) with Cu target and  $K\alpha$  radiation ( $\lambda=0.154$  nm) at 40 kV and 50 mA. The scanning rate was  $0.5^\circ/\text{min}$  and the scanning scope of  $2\theta$  was  $1\text{--}10^\circ$  at room temperature.

The surface morphology of the microspheres was investigated by using SEM (Hitachi, S-750, Japan). Freeze-dried microspheres were coated with a thin layer of gold and photographed in the electron microscope.

### 2.4. Batch adsorption studies

The batch adsorption experiments in duplicate were carried out. Adsorption experiments were conducted in 250-mL flasks containing 100 mL of  $\text{Cu}^{2+}$  solution using 0.1 g chitosan/REC nanocomposite microspheres as adsorbent. The bottles were agitated at 120 rpm in a thermostatic shaking incubator to reach the equilibrium. The effect of initial copper concentration was studied in the range of 50–1,000 mg/L at pH 4.7 at room temperature for 12 h.

The effect of contact time on adsorption capacity was studied in the range 30–720 min at an initial copper concentration of 600 mg/L at pH 4.7 at room temperature. The effect of initial pH on adsorption capacity was studied by varying solution pH from 3 to 4.7 at an initial copper concentration of 600 mg/L for 5 h at room temperature. The solution pH was adjusted with dilute HCl or NaOH solution. The effect of temperature competitor was carried out at an initial copper concentration of 600 mg/L at pH 4.7 under varying temperature (15–55°C) for 5 h.

After adsorption, the solutions were filtered and the concentrations of Cu(II) were determined by a GGX-9 atomic absorption spectrometer (Haiguang, China). The adsorption capacity ( $Q$ ) was calculated as:

$$Q = \frac{(C_0 - C) \times V}{1000 m} \quad (1)$$

where  $C_0$ ,  $C$ , respectively, represent the concentration ( $\text{mg L}^{-1}$ ) of metal ions in solution before and after adsorption,  $V$  is the volume (mL) of metal ions solution,  $m$  is the quality (g) of dry microspheres.

### 3. Results and discussion

#### 3.1. Characterization of chitosan/REC nanocomposite microspheres

As shown in Fig. 1, the characteristic peaks of REC are as follows: Si-O bend vibration adsorption of 476–545  $\text{cm}^{-1}$ , -OH vibration band of 910 and 3,436  $\text{cm}^{-1}$ , Si-O stretching vibration adsorption of 1,020 and 1,050  $\text{cm}^{-1}$ . In the characteristic peaks of CTS, the

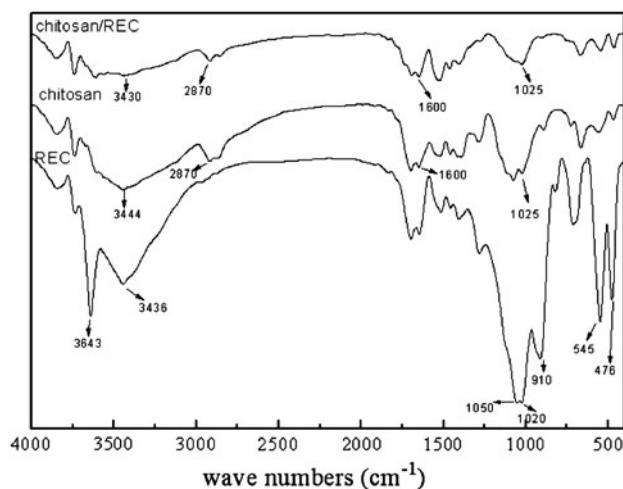


Fig. 1. FT-IR spectra of chitosan, REC, and chitosan/REC nanocomposite microspheres.

absorption band at 1,600  $\text{cm}^{-1}$  attributes to N-H bending mode of  $-\text{NH}_2$ , and the absorption peaks associated to N-H bonding to O-H are at 3,444  $\text{cm}^{-1}$ . The spectra of chitosan/REC microspheres show that the characteristic peaks of both chitosan and REC occur in the spectra of the composite, which are the combination of chitosan with REC. The difference is that the broad band at 3,430  $\text{cm}^{-1}$ , which is stretching vibrations of hydroxyl, amino and amide groups, shifts to the lower frequency, and becomes broader and weaker or even disappears, which indicates that  $-\text{NH}_2$  and  $-\text{OH}$  groups of chitosan formed hydrogen bonds with the  $-\text{OH}$  group in REC which coincided with the chitosan/REC composites [10]. Besides, hydrogen bonding may take place between the chitosan molecules and inside the chitosan molecules, and it was reported that  $-\text{OH}$  groups in REC surface were able to interact immensely with the polymer substrate to form new interface layer or partly network structure [11].

Fig. 2 shows that the XRD patterns of REC and chitosan/REC nanocomposite microspheres. The interlayer distance of REC can be calculated by Bragg equation:  $\lambda = 2d \sin \theta$ . It can be observed that unmodified rectorite exhibits  $2\theta = 3.49^\circ$  and the interlayer distance is 2.53 nm. Compared with REC, the diffraction peak of chitosan/REC nanocomposite microspheres shifts to the small-angle after modified by chitosan, the interlayer distance increased to 3.01 nm. This result indicated that the chitosan has intercalated into the gallery of REC and formed a new composite material, which is in accordance with the previous report [12].

Fig. 3 shows the images of the chitosan/REC nanocomposite microspheres. It can be seen that the well-shaped particles with diameter about 170  $\mu\text{m}$  were

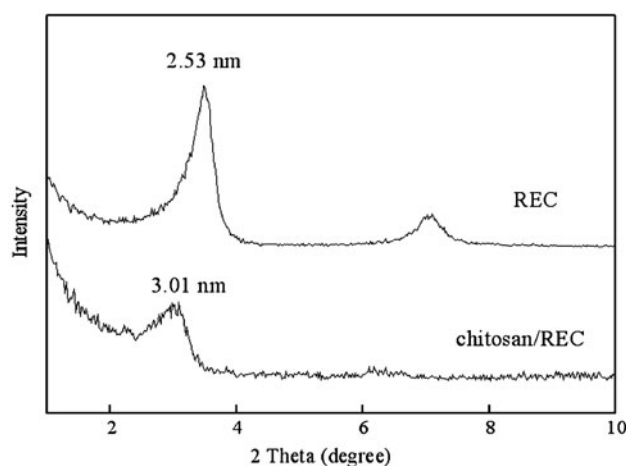


Fig. 2. XRD patterns of REC and chitosan/REC nanocomposite microspheres.

achieved. The microspheres are the rules of spherical and displayed a smooth surface. Microporous structure of microspheres is not obvious, which will slow down the diffusion speed of  $\text{Cu}^{2+}$  from surface to inner part of the microspheres. It indicated that add some porogen during the preparation process of the microspheres may improve the adsorption capacity for  $\text{Cu}^{2+}$ .

### 3.2. Effect of Initial $\text{Cu}^{2+}$ Concentration on adsorption

The adsorption is greatly influenced by the concentration of the solution, as the adsorptive reactions are directly proportional to the concentration of the solute. The effect of the initial concentration on  $\text{Cu}^{2+}$  adsorption was carried out by vibrating 100 mL various  $\text{Cu}^{2+}$  concentrations of copper sulfate solution (pH 4.7) and adding 0.1 g adsorbent at room temperature for 12 h.

It can be seen from Fig. 4 that the adsorption capacity increased from 30.6 to 187.5 mg/g with the increase of initial  $\text{Cu}^{2+}$  concentration from 50 to 600 mg/L. Thereafter, the adsorption of  $\text{Cu}^{2+}$  exhibited to reach equilibrium. The results can be attributed to that there are many  $-\text{OH}$  groups and  $-\text{NH}_2$  groups (binding sites) on chitosan/REC nanocomposite microspheres, which mainly decided the adsorption capacity of  $\text{Cu}^{2+}$ . In terms of the mechanism for the adsorption of copper ions on chitosan beads, there are two different opinions on the interaction between chitosan and  $\text{Cu}^{2+}$ . One proposes that four amino ( $-\text{NH}_2$ ) groups on chitosan chains serve as coordination sites interacting with  $\text{Cu}^{2+}$ . And the other one believes that it is two amino ( $-\text{NH}_2$ ) groups and two hydroxyl ( $-\text{OH}$ ) groups that coordinate with  $\text{Cu}^{2+}$  [13]. There-

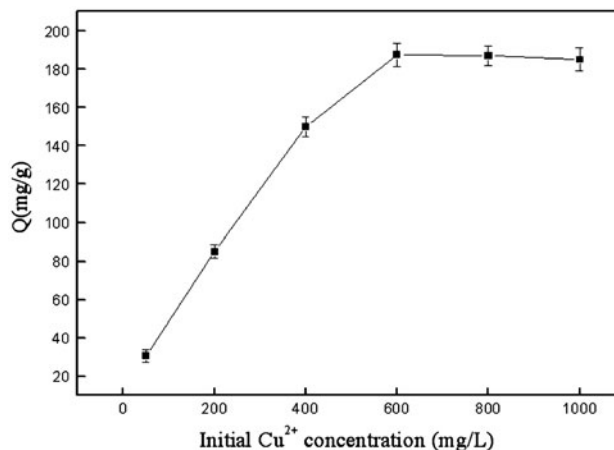


Fig. 4. Effect of initial  $\text{Cu}^{2+}$  concentration on adsorption.

fore, at the lower initial  $\text{Cu}^{2+}$  concentration, the ratio of initial number of  $\text{Cu}^{2+}$  to the  $-\text{OH}$  groups and  $-\text{NH}_2$  groups on the adsorbent is low and  $-\text{OH}$  groups and  $-\text{NH}_2$  groups might have some surplus after chelated with  $\text{Cu}^{2+}$ . However, in case of higher initial  $\text{Cu}^{2+}$  concentration, the adsorption capacity increased slowly and even achieve the equilibrium, this is because that the number of  $-\text{OH}$  groups and  $-\text{NH}_2$  groups on the adsorbent is constant, the adsorbent could not adsorb  $\text{Cu}^{2+}$  when binding sites not enough.

### 3.3. Effect of contact time on adsorption

Contact time studies are helpful in understanding the amount of  $\text{Cu}^{2+}$  adsorbed at various time intervals by a fixed amount of the adsorbent. In the test for investigation of the effect of contact time on adsorption of  $\text{Cu}^{2+}$ , 0.1 g adsorbent and 100 mL copper

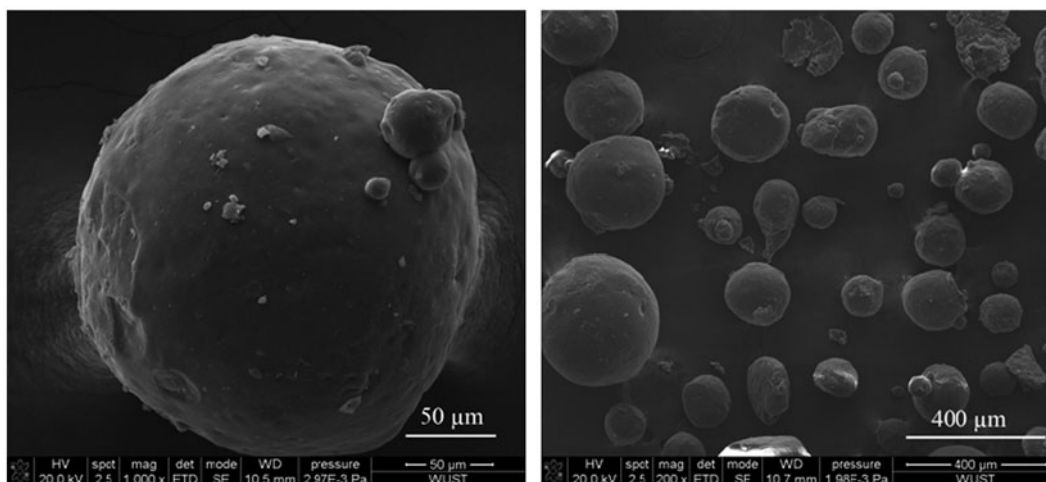


Fig. 3. SEM images of the chitosan/REC nanocomposite microspheres.

sulfate solution (pH 4.7, initial concentration  $600 \text{ mg L}^{-1}$ ) were used, and the test was carried out at room temperature. The results are described in Fig. 5, the adsorption capacity sharply increased within 180 min and then gradually increased with further prolonging the contact time until equilibrium. The main reason of this adsorption rate was that the adsorbent had a large number of active binding sites for  $\text{Cu}^{2+}$  absorption during the initial stage of the treatment time. However, the adsorption capacity of  $\text{Cu}^{2+}$  became slower in latter stages. It can be attributed to the great decrease of the binding sites on the surface of chitosan/REC nanocomposite microspheres. As the previous research [14], when binding sites are not enough for chelating with  $\text{Cu}^{2+}$ , pore diffusion or intraparticle diffusion then take place which allows adsorbates to diffuse from the surface to inner part of the adsorbent. Under our experimental conditions, the equilibrium time for the adsorption of  $\text{Cu}^{2+}$  onto chitosan/REC nanocomposite microspheres is 300 min. The maximal  $\text{Cu}^{2+}$  uptake by chitosan/REC nanocomposite microspheres was  $190.2 \text{ mg g}^{-1}$ .

#### 3.4. Effect of pH on adsorption

The effect of pH on the adsorption of  $\text{Cu}^{2+}$  was investigated at the room temperature. The solutions were adjusted to pH 3–4.7 (natural pH of copper sulfate solution) with copper sulfate solution (initial concentration  $600 \text{ mg L}^{-1}$ ) and stirred for 5 h at room temperature. The results are shown in Fig. 6. It appeared that the adsorption capacity increased with increasing contact pH and the maximum uptake of  $\text{Cu}^{2+}$  took place at pH 4.7. The maximum uptake was  $187.25 \text{ mg g}^{-1}$ . It was observed that the adsorption is highly dependent on the pH of the solution, which

affects the surface charge of the adsorbent and the degree of ionization of the adsorbate. At lower pH, more protons will be available and more  $-\text{NH}_2$  groups of the microspheres become protonated ( $-\text{NH}_3^+$ ). As  $\text{Cu}^{2+}$  is transported from the solution to the adsorbent, the protonated amino groups inhibit the approach of  $\text{Cu}^{2+}$  due to the electrostatic repulsion force exerted by  $-\text{NH}_3^+$  on the adsorbent surface [15]. Therefore, the adsorption capacity of  $\text{Cu}^{2+}$  was at a low level. When the pH is increased from pH 3 to 4.7, the  $-\text{NH}_2$  groups become deprotonated, hence there are enough binding sites to bind with  $\text{Cu}^{2+}$ . At pH value higher than 4.7, the  $\text{Cu}^{2+}$  will be precipitated in the form of  $\text{Cu}(\text{OH})_2$ , which will decrease the concentration of  $\text{Cu}^{2+}$  in solution and influence the accuracy of the experiment.

#### 3.5. Effect of temperature on adsorption capacity and adsorption thermodynamics

The effect of temperature on  $\text{Cu}^{2+}$  removal was carried out in the 100 mL copper sulfate solution (pH 4.7,  $600 \text{ mg/L}$ ) by adding 0.1 g adsorbent under vary temperature ( $15\text{--}55^\circ\text{C}$ ) for 5 h. Thermodynamic parameters such as standard Gibbs free energy change ( $\Delta G^0$ ), standard enthalpy  $\Delta H^0$ , and standard entropy change ( $\Delta S^0$ ) were calculated as follows. The change in free energy of sorption is given by:

$$\Delta G^0 = -RT \ln K_c \quad (2)$$

Standard enthalpy,  $\Delta H^0$ , and standard entropy,  $\Delta S^0$ , of adsorption can be estimated from van't Hoff equation given in:

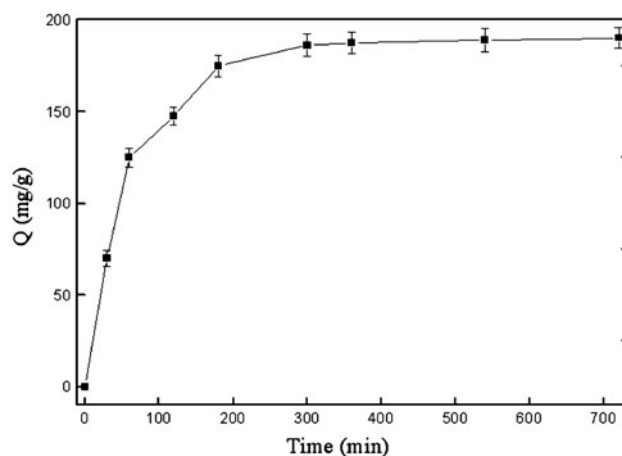


Fig. 5. Effect of contact time on adsorption.

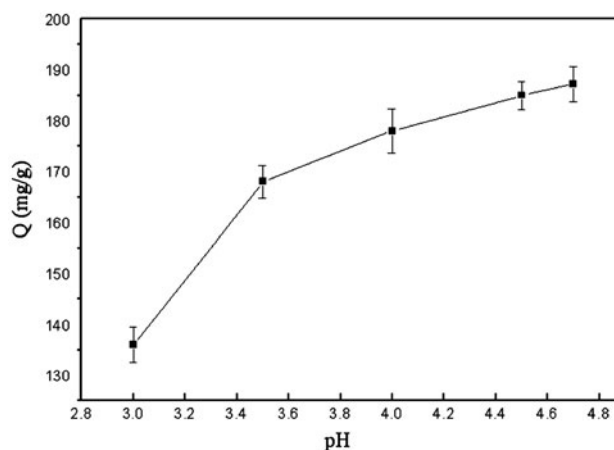


Fig. 6. Effect of pH on adsorption.

$$\ln K_c = \frac{-\Delta H^0}{RT} + \frac{\Delta S^0}{R} \quad (3)$$

where  $R$  is the gas constant,  $K_c$  is adsorption equilibrium constant. The  $K_c$  value is calculated from the equation [16]:

$$K_c = \frac{(Q_0 - Q_c)}{Q_c} \times \frac{V}{m} \quad (4)$$

where  $Q_0$  is the initial concentration of the  $\text{Cu}^{2+}$  in solution ( $\text{mg L}^{-1}$ ) and  $Q_c$  is the equilibrium concentration of the  $\text{Cu}^{2+}$  in the solution ( $\text{mg L}^{-1}$ ).  $V$  (mL) is the volume of  $\text{Cu}^{2+}$  solution and  $m$  is the quality (g) of dry microspheres.

Table 1 shows that the uptake of  $\text{Cu}^{2+}$  by chitosan/REC nanocomposite microspheres appears to increase between 15 and 45°C. This might be due to the possibility of an increase in the porosity and in the total pore volume of the adsorbent, an increase in the number of active sites for adsorption. Also, the rate of diffusion of the adsorbate molecules across the external boundary layer and in the internal pores of the adsorbent increased with increasing temperature [17]. However, a higher temperature (>45°C) favors dechelation, which leads to a decrease in the adsorption capacity of  $\text{Cu}^{2+}$ . This result is very similar to the previous work [18].

The thermodynamic parameters are shown in Table 1; the negative values of  $\Delta G^0$  at different temperatures indicate the spontaneous nature of the adsorption process. The positive value of  $\Delta S^0$  suggests the increased randomness at the solid/solution interface during the adsorption of  $\text{Cu}^{2+}$  onto chitosan/REC nanocomposite microspheres. The positive value of  $\Delta H^0$  for the copper removal indicates the endothermic nature of sorption process. A similar behavior was also found for the removal of copper(II) using chitin/chitosan nano-hydroxyapatite composite [19].

Table 1  
Effect of temperature on adsorption and thermodynamic parameters

Temperature (°C)	Adsorption capacity (mg/g)	$\Delta G^0$ (kJ/mol)	$\Delta H^0$ (kJ/mol)	$\Delta S^0$ (kJ/molK)
15	109.2	-1.870	22.285	0.085
25	175.5	-3.434		
35	194.2	-3.923		
45	214.6	-4.435		
55	161.8	-3.471		

### 3.6. Equilibrium isotherm models

The equilibrium isotherm equations could be used to describe the experimental sorption data and provide some insight into the sorption mechanism, the surface properties, and the affinity between sorbent and sorbate [20]. The Langmuir isotherm model is usually used for monolayer adsorption onto a surface with finite number of identical sites. The Freundlich isotherm model assumes multilayer adsorption with a heterogeneous energetic distribution of active sites on surface.

Langmuir isotherm equation,

$$\frac{1}{Q_e} = \frac{1}{Q_{\max}} + \frac{1}{BQ_{\max}C_e} \quad (5)$$

where  $C_e$  ( $\text{mg L}^{-1}$ ) is the equilibrium concentration of metal ion;  $Q_e$  ( $\text{mg g}^{-1}$ ) is the sorption capacity of metal ion;  $Q_{\max}$  ( $\text{mg g}^{-1}$ ) is the maximum adsorption capacity of the adsorbent;  $B$  is the Langmuir adsorption constant.

Freundlich isotherm equation,

$$\ln Q_e = \ln K + \left(\frac{1}{n}\right) \ln C_e \quad (6)$$

where  $C_e$  ( $\text{mg L}^{-1}$ ) is the liquid-phase  $\text{Cu}^{2+}$  concentration at equilibrium,  $K$  is the Freundlich isotherm constant, and  $1/n$  (dimensionless) is the heterogeneity factor, respectively.

The equilibrium isotherm was determined using batch studies. In the experiments, 0.1 g of adsorbent was added to 100 mL solution of copper concentration between 50 and 1,000 mg/L, pH 4.7, in a thermostatic shaking incubator, for 12 h, at room temperature. After adsorption, the adsorption capacity ( $Q$ ) was calculated by Eq. (1), and Freundlich and Langmuir model's parameters were calculated by Eq. (5) and (6). Table 2 shows the value of calculated parameters. The values of  $R^2$  of Langmuir and Freundlich models are 0.9879 and 0.9406, respectively. And the maximum sorption capacity calculated from Langmuir isotherm was  $201.6 \text{ mg g}^{-1}$ , which was close to the experimental values. It can be concluded that the Langmuir isotherm best represents the equilibrium adsorption of

Table 2  
Freundlich and Langmuir isotherm constants

Freundlich adsorption model			Langmuir adsorption model		
$n$	$K$	$R^2$	$Q_{\max}$ (mg/g)	$B$	$R^2$
1.9724	7.4989	0.9406	201.6	0.0027	0.9879

Table 3  
Dynamics constant of two models

Adsorption capacity $q_{e(\text{exp})}$ ( $\text{mg g}^{-1}$ )	Pseudo-first-order kinetics			Pseudo-second-order kinetics		
	$K_1$	$q_{e(\text{cal})}$ ( $\text{mg g}^{-1}$ )	$R^2$	$K_2$	$q_{e(\text{cal})}$ ( $\text{mg g}^{-1}$ )	$R^2$
186.25	$7.35 \times 10^{-3}$	82.71	0.3991	$0.105 \times 10^{-3}$	209.5	0.9883

$\text{Cu}^{2+}$  onto chitosan/REC nanocomposite microspheres, which suggests the monolayer coverage of the dye on the surface of the adsorbent.

### 3.7. Kinetic modelings

In order to investigate the adsorption kinetics, two different kinetics models, pseudo-first-order and pseudo-second-order rate models were used in this study. The pseudo-first- and pseudo-second-order models are given by:

$$\log(q_e - q_t) = \log q_e - \frac{k_1}{2.303} \times t \quad (7)$$

The pseudo-second-order rate equation is represented as:

$$\frac{t}{q_t} = \frac{1}{k_2 q_e^2} + \frac{t}{q_e} \quad (8)$$

where  $q_e$  and  $q_t$  ( $\text{mg g}^{-1}$ ) are the amounts of  $\text{Cu}^{2+}$  adsorbed onto adsorbents at equilibrium and at time  $t$ , respectively.  $k_1$  (1/min) and  $k_2$  ( $\text{g/mg min}$ ) are the rate constant of pseudo-first- and second-order adsorption, respectively.

The kinetic studies were performed using 0.1 g of adsorbent in 100 mL of copper solution at initial concentration of 600 mg/L. The flasks were agitated at 120 rpm for pre-determined time intervals (30–720 min). After adsorption, the adsorption capacity ( $Q$ ) was calculated by Eq. (1), and the parameters of the pseudo-first-order and second-order kinetics were calculated by Eqs. (7) and (8). Table 3 shows the value of calculated parameters. The maximum sorption capacity calculated from the pseudo-second-order rate equation was  $209.5 \text{ mg g}^{-1}$  which was close to the experimental values. On comparing the  $R^2$  values and  $q_{e(\text{cal})}$  obtained, it can be easily concluded that the adsorption reaction proceeds via a pseudo-second-order mechanism rather than a pseudo-first-order mechanism. It indicates that the sorption behavior may involve valency forces through electron sharing between the metal ions and adsorbent [21], and chemisorption might be the rate-limiting step that controls the adsorption process.

## 4. Conclusion

In the work, chitosan/REC microspheres were prepared and characterized. The interlayer distance of REC was enlarged from 2.53 to 3.01 nm. The adsorption tests of  $\text{Cu}^{2+}$  onto chitosan/REC microspheres were carried out. The results showed that the  $\text{Cu}^{2+}$  adsorption process is dependent on pH, contact time, initial  $\text{Cu}^{2+}$  concentration, and temperature. Adsorption kinetics and equilibrium isotherms studies indicated that the sorption processes were better fitted by pseudo-second-order equation and Langmuir equation, respectively. Adsorption thermodynamics study indicated the spontaneous nature and endothermic of the adsorption process.

## Acknowledgement

Contract grant sponsor: National Natural Science Foundational of China (50904047); Wuhan Science and Technology Bureau (201271031420); Hubei Biomass-Resource Chemistry and Environmental Biotechnology Key Laboratory, Wuhan University (HBRCEBL2011-2012002).

## Reference

- [1] K.J. Yao, M. Song, D.J. Hourston, D.Z. Luo, Polymer/Layered Clay Nanocomposites: 2 Polyurethane Nanocomposites, Polymer 43 (2002) 1017–1020.
- [2] S. Kim, E.J. Hwang, Y. Jung, M. Han, S.J. Park, Ionic conductivity of polymeric nanocomposite electrolytes based on poly(ethylene oxide) and organo-clay materials, Colloid Surf. A. 313 (2008) 216–219.
- [3] E.P. Giannelis, R. Krishnamoorti, E. Manias, Polymer-Silicate Nanocomposites: Model Systems for Confined Polymers and Polymer Brushes, Adv. Polym. Sci. 138 (1999) 107–147.
- [4] X.Y. Ma, H.J. Lu, G.Z. Liang, H.X. Yan, Rectorite/thermoplastic polyurethane nanocomposites: Preparation, characterization, and properties, J. Appl. Polym. Sci. 93 (2004) 608–614.
- [5] T. Feng, F. Zhang, J. Wang, L. Wang, Application of Chitosan-Coated Quartz Sand for Congo Red Adsorption from Aqueous Solution, J. Appl. Polym. Sci. 125 (2012) 1766–1772.
- [6] H. Radnia, A.A. Ghoreyshi, H. Younesi, G.D. Najafpour, Adsorption of Fe(II) ions from aqueous phase by chitosan adsorbent: equilibrium, kinetic, and thermodynamic studies, Desalin. Water. Treat. 50 (2012) 348–359.
- [7] V.N. Tirtom, A. Dincer, S. Becerik, T. Aydemir, A. Celik, Removal of lead (II) ions from aqueous solution by using crosslinked chitosan-clay beads, Desalin. Water. Treat. 39 (2012) 76–82.
- [8] P. Monvisade, P. Siriphannon, Chitosan intercalated montmorillonite: Preparation, characterization and cationic dye adsorption, Appl. Clay Sci. 42 (2009) 427–431.

- [9] S. Kittinaovarat, P. Kansomwan, N. Jiratumnukul, Chitosan/modified montmorillonite beads and adsorption Reactive Red 120, *Appl. Clay Sci.* 48 (2009) 87–91.
- [10] S.F. Wang, L. Shen, Y.J. Tong, L. Chen, I.Y. Phang, P.Q. Lim, T.X. Liu, Biopolymer chitosan/montmorillonite nanocomposites: Preparation and characterization, *Polym. Degrad. Stab.* 90 (2005) 123–131.
- [11] X. Wang, Y. Du, J. Yang, X. Wang, X. Shi, Y. Hu, Preparation, characterization and antimicrobial activity of chitosan/layered silicate nanocomposites, *Polymer* 47 (2006) 6738–6744.
- [12] X.Y. Wang, X.F. Pei, Y.M. Du, Y. Li, Quaternized chitosan/rectorite intercalative materials for a gene delivery system, *Nanotechnology* 19 (2008) 375102.
- [13] F. Zhao, B. Yu, Z. Yue, T. Wang, X. Wen, Z. Liu, C. Zhao, Preparation of porous chitosan gel beads for copper(II) ion adsorption, *J. Hazard. Mater.* 147 (2007) 67–73.
- [14] W.S.W. Ngah, N.F.M. Ariff, M.A.K.M. Hanafiah, Preparation, Characterization, and Environmental Application of Crosslinked Chitosan-Coated Bentonite for Tartrazine Adsorption from Aqueous Solutions, *Water Air Soil Pollut.* 206 (2010) 225–236.
- [15] L. Jin, R.B. Bai, Mechanisms of lead adsorption on chitosan/PVA hydrogel beads, *Langmuir* 18 (2002) 9765–9770.
- [16] M.S. Chiou, H.Y. Li, Adsorption behavior of reactive dye in aqueous solution on chemical cross-linked chitosan beads, *Chemosphere* 50 (2003) 1095–1105.
- [17] N.S. Rajurkar, A.N. Gokarn, K. Dimya, Adsorption of Chromium(III), Nickel(II), and Copper(II) from Aqueous Solution by Activated Alumina, *Clean-Soil Air Water* 39 (2011) 767–773.
- [18] S. Sun, A. Wang, Adsorption properties of carboxymethyl-chitosan and cross-linked carboxymethyl-chitosan resin with Cu(II) as template, *Sep. Purif. Technol.* 49 (2006) 197–204.
- [19] M.R. Gandhi, G.N. Kousalya, S. Meenakshi, Removal of copper(II) using chitin/chitosan nano-hydroxyapatite composite, *Int. J. Biol. Macromol.* 48 (2011) 119–124.
- [20] B.S. Krishna, D.S.R. Murty, B.S.J. Prakash, Thermodynamics of chromium(VI) anionic species sorption onto surfactant-modified montmorillonite, *J. Colloid Interface Sci.* 229 (2000) 230–236.
- [21] C.M. Niu, W.H. Wu, Z. Wang, S.M. Li, J.Q. Wang, Adsorption of heavy metal ions from aqueous solution by cross-linked carboxymethyl konjac glucomannan, *J. Hazard. Mater.* 141 (2007) 209–214.